Hydrol. Earth Syst. Sci. Discuss., 7, 1621–1654, 2010
www.hydrol-earth-syst-sci-discuss.net/7/1621/2010/

Hydrology and Earth System Sciences Discussions

This discussion paper is/has been under review for the journal Hydrology and Earth System Sciences (HESS). Please refer to the corresponding final paper in HESS if available.

Using flushing rate to investigate spring-neap and spatial variations of gravitational circulation and tidal exchanges in an estuary

D. C. Shaha[1], Y.-K. Cho[1], G.-H. Seo[1], C.-S. Kim[1], and K.-T. Jung[2]

[1]Department of Oceanography, Chonnam National University, Gwangju 500-757, Korea
[2]Korea Ocean Research and Development Institute, Ansan 426-744, Korea

Received: 6 February 2010 – Accepted: 18 February 2010 – Published: 2 March 2010

Correspondence to: Y.-K. Cho (ykcho@chonnam.ac.kr)

Published by Copernicus Publications on behalf of the European Geosciences Union.

Abstract

Spring-neap and spatial variations of gravitational circulation and tidal exchanges in the Sumjin River Estuary (SRE) were investigated using the flushing rate method. This method was applied to multiple estuarine segments to estimate both the exchanges. The strength of gravitational circulation and tidal exchanges modulated significantly between spring and neap tides, where stratification alternated between well-mixed and highly-stratified conditions over the spring-neap cycle. Strong gravitational circulation developed during neap tide along the SRE due to the significant reduction in vertical mixing that accompanied strong stratification. The tidal exchanges dominated over gravitational circulation near the mouth during spring tide due to the larger tidal amplitude that caused well-mixed conditions and rapid exchange. In contrast, the central and inner regimes were found to be partially stratified during spring tide due to the reduction in tidal amplitude which induced gravitational circulation and weakened the tidal exchange. Only the gravitational circulation dominated at the upstream end during spring and neap tides which was governed by the river flow.

1 Introduction

The net flow of water into and out of estuaries influences the exchanges with the surrounding coastal region, thus playing a role in controlling the estuarine environment by regulating the transport of, for instance, nutrients, sediments, planktonic organisms and pollutants. Therefore, it is essential to understand estuarine hydrodynamic processes, such as tidal exchange and gravitational circulation exchange or some combination of the two, which transport water and its constituents (Monsen et al., 2002; Ribeiro, et al., 2004). The tidal exchange is more or less independent of the river discharge, whereas the gravitational circulation exchange is strongly dependent on the freshwater input in maintaining the longitudinal density gradient that controls an exchange flow, with seaward flow at the surface and landward flow at depth (Officer and Kester, 1991; Dyer,

HESSD

7, 1621–1654, 2010

1997). The competition between tidally induced vertical mixing and river generated buoyancy is the main factor determining the differences in water exchange.

Spring-neap variations in tidal shear stress may result in spring-neap variations in tidally driven mixing, stratification and gravitational circulation (Jay and Smith, 1990; Uncles and Stephens, 1996; Monismith et al., 1996; Ribeiro, et al., 2004; Savenije, 2005). Tide-driven shear mechanisms dominate in narrow, shallow estuaries, and strong tidal currents tend to suppress stratification through vigorous mixing, which inhibits gravitational circulation (West and Broyd, 1981; Uncles et al., 1985; Geyer, 1993; Savenije, 2005). However, the weaker turbulence during a neap tide could lead to an acceleration of gravitational circulation (Nunes Vaz et al., 1989; Monismith et al., 1996). Such influence of low mixing at neap tides was noted by Jay and Smith (1990) in the extent of salt intrusion into the Columbia River Estuary.

Gravitational circulation is the most efficient mechanism for flushing river-borne pollutants out to the open sea (Nunes Vaz et al., 1989). Where gravitational circulation does not occur, behavioral mechanisms can still reduce dispersive and advective losses. In some estuaries, gravitational circulation may increase in strength with increasing river flow, which cause an advective loss of estuarine resident populations from their maintenance position, particularly larval forms of benthic or demersal organisms, but also copepods and larval fish (Hough and Naylor, 1991; Jassby, et al., 1995; Morgan et al., 1997, Kimmerer et al., 1998; Kimmerer et al., 2002; Monismith et al., 2002). Recently, the spatiotemporal variations on the abundance of the demersal copepod *Pseudodiaptomus* sp. in the Sumjin River Estuary (SRE) have been reported (Park et al., 2005). However, there has been no information on the physical aspects of the tide-driven exchanges and gravitational circulation exchanges for the SRE.

Officer and Kester (1991) apply the flushing rate method to estimate the tide-driven exchanges and gravitational circulation exchanges for an estuary. They use a single transport time scale which is the flushing rate for the entire estuarine system. However, Monsen et al. (2002) reported that no single transport time scale for a system is valid for all time periods, locations and constituents, and it does not describe all transport

processes. In addition, a single transport time scale provides no information about the connections between transport and spatial heterogeneity of non-conservative quantities, such as specific conductivity, temperature and chlorophyll a. As a single transport time scale does not represent the spatial variation of all transport processes, the flushing rate method was applied to multiple segments of the SRE to examine the spatial variability of transport time scales and to estimate gravitational circulation and the tidal exchange.

The main focuses of this study are (i) to understand the spatial variation of gravitational circulation and tide-driven exchanges during spring and neap tides in multiple segments of the SRE on the basis of the flushing rate and; (ii) to suggest the flushing rate as an useful parameter to investigate the relative strength of the tide-driven exchanges and gravitational circulation exchanges in an estuary.

The rest of this paper is organized as follows. The data sources are briefly presented in Sect. 2. The methodology is described in Sect. 3. The results are presented in Sect. 4. A discussion follows in Sect. 5, with the conclusions in Sect. 6.

2 Study area and data

The SRE is one of the few natural estuaries on the south coast of Korea. The watershed area, including farmland, is almost 4897 km^2. The Sumjin River discharges into Gwangyang Bay. The bay is connected to the south to the coastal ocean (South Sea) and to the east to Jinjoo Bay via the narrow Noryang Channel (Fig. 1). The climate of Korea is characterized by four distinct seasons: spring (March, April, May), summer (June, July, August), autumn (September, October, November) and winter (December, January, February). The annual mean precipitation is 1418.4 mm, based on annual data from 1968 to 2001. Seasonal precipitation and runoff in the Sumjin River basin have decreased in spring and winter, but increased in summer (Bae et al., 2008). The tidal cycle is semi-diurnal, with mean spring and neap ranges of 3.33 and 1.02 m, respectively.

HESSD
7, 1621–1654, 2010

The river discharge data used in this study were from the Songjung gauge station, located about 11 km upstream from CTD (conductivity-temperature-depth) station 24 operated by the Ministry of Construction and Transportation. The maximum monthly median river discharge was highest (370 $m^3 s^{-1}$) in July 2006 and lowest (11 $m^3 s^{-1}$) in January 2005. Tidal constituents for Gwangyang bay (GT2, Fig. 1) were obtained from the Korean Ocean Research & Development Institute (http://www.kordi.re.kr/odmd/harmonic2004/). The M_2 tide is the primary tidal constituent at the river mouth. Sea level data for 2005 and 2006 from Hadong tidal (HT) gauge station (http://www.wamis.go.kr/wkw/WL_DUBWLOBS.ASPX) were analyzed using the Task-2000 tidal package developed by the Proudman Oceanographic Laboratory (Bell et al., 1999). The major tidal constituents (M_2, S_2, K_1, O_1) are shown in Table 1. The tidal amplitudes of the M_2 and S_2 constituents were found to decrease to 12 and 8% within the estuary at HT, respectively.

Time-series observations of the salinity distribution were conducted over a tidal cycle during spring tide, with the highest water level being approximately 3.66 m at station 7 on 21–22 July 2005. To obtain complete features of the spring-neap variation in time-depth salinity distribution, observations were repeated over a tidal cycle at the same station during spring tide on 15–16 June and during neap tide on 21–22 June 2006. The longitudinal transects for salinity and temperature were carried out at high water during both spring and neap tides during each season from August 2004 to April 2007 using a CTD profiler (Ocean Seven 304 of IDRONAUT Company). A Global Positing System was used to obtain the locations of the CTD stations (Fig. 1). The nominal distance between the CTD stations was 1 km. The measurements were started from the river mouth one hour before high water, and took about one hour to complete. On the basis of the stratification parameter, which is the ratio of the difference in salinity between the surface and bottom divided by the depth averaged salinity, well-mixed conditions were found near the mouth of the SRE, with partially-mixed conditions in the central and inner regimes during spring tide. In contrast, strong stratified conditions were found along the SRE during neap tide (Shaha and Cho, 2009).

3 Methods

The flushing rate was calculated for multiple estuarine segments in response to the daily average freshwater input. Bathymetric data were collected from the Regional Construction and Management Office of the Construction Department, the Ministry of Construction. Pilson (1985) reported that an increase in depth increases the flushing time. Mean sea level depth was converted to approximate high water depth by the addition of the half-tide height for both spring and neap tides. The Extended Trapezoidal, Extended Simpson's and Extended Simpson's 3/8 Rules were used to determine the volume (V_i) of each segment for both spring and neap tides (Press et al., 1988). The difference in the volume calculated by the three different methods indicates the accuracy of the volume calculations. If the three volume calculations are reasonably close together, the true volume is close to these values. When the three values differed by more than 5%, a finer grid was determined before performing the volume calculations again. This approach has been explained in detail by Press et al. (1988).

Four CTD stations were allocated for each segment of approximately 4 km long. Mean salinity values for each segment (S_i) were calculated from the mean of each station, using the vertical salinity profiles of the four CTD stations on each survey day. The salinity of the seawater entering the SRE via the Gwangyang Bay varied with time. The CTD station 1 was selected as a reference salinity of the seawater (S_{sw}) entering in the bottom of the estuary mouth for each survey day.

The freshwater fraction method involves the calculation of the freshwater volume of each segment at high tide using the freshwater fraction formula as follows (Williams, 1986; Dyer, 1997):

$$f_i = 1 - \frac{S_i}{S_{sw}} \quad (1)$$

where i is the segment number, f_i the freshwater fraction or freshwater content of each segment, S_{sw} the salinity of seawater entering in the bottom of the estuary mouth and S_i the mean salinity of each segment. The volume of freshwater (V_f) for each segment

HESSD
7, 1621–1654, 2010

is calculated by multiplying the freshwater fraction (f_i) by the volume of each segment (V_i), which is described by:

$$V_{f_i} = f_i V_i \tag{2}$$

where V_i is the high tide volume of each segment.

The flushing times were successfully calculated using the freshwater fraction method for multiple estuarine segments (Williams, 1986). Sheldon and Alber (2002, 2006) also suggested that the freshwater fraction method can easily be applied to multiple estuarine segments, because the flushing time for an entire estuary is the sum of the segment flushing times. Flushing time is then given by:

$$T_i = \frac{V_{f_i}}{R} \tag{3}$$

where T_i is the flushing time of each estuarine segment and R the freshwater discharge.

The flushing rate (F) is the rate at which the freshwater is exchanged with the open seawater (Officer and Kester, 1991; Dyer, 1997) and is defined for multiple estuarine segments as follows:

$$F_i = \frac{V_i}{T_i} = \frac{R}{f_i} \tag{4}$$

The quantity, F, which has the dimensions of $m^3\,s^{-1}$, represents the combined effects of the diffusive tidal exchanges and the advective gravitational circulation exchanges, which together equal the total longitudinal flux in the Hansen-Rattray estuarine parameter $\boldsymbol{\nu}$ (Hansen and Rattray, 1965, 1966). The tidal exchange should be independent of the river discharge, but the gravitational circulation exchanges will depend strongly on it (Officer and Kester, 1991; Dyer, 1997). If the tidal exchanges are dominant over the gravitational circulation, then the flushing rate (F) should be about constant for all river discharges (Dyer, 1997). If there were no tidal exchanges, a plot of F against R will give

a curve with an intercept at zero and increasing values of F for increasing values of R (Dyer, 1997). If both tidal exchanges and gravitational circulation exchanges are operative, the plot of the flushing rate against the river discharge should have an intercept value (F_{int}) at zero river flow, which represents the tidal exchange, and the amounts in excess of the intercept value represent the gravitational circulation exchange (G_c) (Officer and Kester, 1991; Dyer, 1997). The tide-driven exchanges are dominant over gravitational circulation exchanges when $F_{int} > G_c$, and the gravitational circulation exchanges over tide-driven exchanges when $F_{int} < G_c$.

The estuarine parameter $\boldsymbol{\nu}$ can then be defined as (Officer and Kester, 1991; Dyer, 1997)

$$\boldsymbol{\nu} = \frac{F_{int}}{F} \tag{5}$$

and reflects the relative importance of tide-driven dispersion versus the total longitudinal dispersion. For $\boldsymbol{\nu} \sim 1$, tide-driven exchange processes are dominant. For $\boldsymbol{\nu} \sim 0$, gravitational circulation processes are dominant.

4 Results

4.1 Diurnal variation of salinity

A time-series of salinity was first observed over a tidal cycle during spring tide at CTD station 7 on 21–22 July 2005. The mean river discharge over the M_2 tidal cycle was $28\,m^3\,s^{-1}$. During high tide, a salinity of 27 psu was found at the observation point (Fig. 2a). The difference in salinity between two subsequent high tides was approximately 3 psu due to variation in the tidal amplitude. Two more time series were taken at station 7 over the M_2 tidal cycle during spring tide on 15–16 June and during neap tide on 21–22 June 2006. The mean river discharge over the tidal cycle during spring tide was $120\,m^3\,s^{-1}$. Comparing this distribution with the previous spring tide time-depth

salinity distribution, it appeared that the buoyancy force as a freshwater input was the main differentiating factor. The flood phase was longer (>5 h) compared to ebb phase (~2.5 h), as the bed shear counteracts the estuarine circulation during a flood and acts together with estuarine circulation during an ebb (Fig. 2b). However, a salinity of 27 psu was again found at the observation point during the high tide when the river discharge was 77% larger than that in July 2005. This increased river discharge did not hinder the inflow of the 27 psu salt wedge from Gwangyang Bay to the same observation point. However, the vertical salinity gradient at high water during spring tide increased by 50% in 2006 than that in 2005. During neap tide, the river discharge and tidal amplitude were 18 $m^3 s^{-1}$ and 0.86 m, respectively. The difference in the vertical salinity at high water during neap tide was smaller (9 psu) due to an 85% lower river discharge than that during spring tide (24 psu) (Fig. 2b and c).

4.2 Longitudinal variation of salinity

Tide and river discharge are two main forcing factors controlling estuarine circulation (deCastro et al., 2004; Savenije, 2005; Ji, 2008). Changes in the tidal currents with the spring-neap tidal cycle can result in fortnightly modulation of stratification and gravitational circulation (Simpson, et al. 1990; Ribeiro, et al., 2004). Longitudinal transects of salinity were carried out at high water during both spring and neap tides in each season from August 2004 to April 2007. The vertical sections showed a relatively well mixed to partially mixed structure during spring tide (Figs. 3 and 4). The highest saline water of 33 psu appeared at the lower portion of the estuary over the entire observation periods during spring, 2005 (Fig. 4b). In addition, an isolated structure of saline water appeared about 9 km upstream from the mouth (Fig. 4d, g and h). This phenomenon may have occurred due to mixing between seawater and freshwater inflow from the tributary (Hwangchon), as the density structure is largely controlled by the freshwater input in the coastal water and the density structure followed that salinity distribution. The vertical sections of salinity (2006, 2007) during spring and neap tides have not been shown here owing to their similar structures.

Strong stratification appeared during neap tide in all seasons (Figs. 3 and 4). As the tidal amplitude decreased during neap tide, the weakened effect of the bottom friction strengthens the gravitational circulation, causing strong stratification. Strong stratification and gravitational circulation during neap tide was noted by Monismith et al. (1996) in Northern San Francisco Bay. On the basis of the stratification parameter, the SRE transitions from partially or well-mixed during spring tide to stratified during neap tide (Shaha and Cho, 2009). In general, the strength of stratification was comparatively increased in summer due to the high river discharge (77 $m^3 s^{-1}$) compared to the other seasons (Fig. 4g).

4.3 Spring-neap and spatial variations of gravitational circulation exchanges and tide-driven exchanges

To investigate the spatial variations in gravitational circulation exchanges and tide-driven exchanges during spring and neap tides, the flushing rate was calculated by dividing the SRE into six segments. Figure 5 depicts the temporal variations in the flushing rate during spring and neap tides. The flushing rate ranged between 428 and 990 $m^3 s^{-1}$ in SEG1 during spring tide, whereas from 123 to 547 $m^3 s^{-1}$ during neap tide. The flushing rates decreased to ~11 and ~12 $m^3 s^{-1}$ during spring and neap tides at the upstream end (SEG6), respectively. Figure 6 shows the spatial variations in the mean flushing rate during spring and neap tides. The mean flushing rate was extremely heterogeneous, ranging from 27 to 742 $m^3 s^{-1}$, depending on the location. The flushing rate was approximately two times greater during spring tide (~742 and 236 $m^3 s^{-1}$) due to the larger tidal amplitude than during neap tide (~279 and 129 $m^3 s^{-1}$) in SEG1 and SEG2, respectively. The flushing rate increased in the central and inner regimes during neap tide relative to the spring tide due to enhancing the gravitational circulation (SEG4 and SEG5). In SEG6, the flushing rates were approximately the same (~27 $m^3 s^{-1}$) during spring and neap tides, indicating that the flushing rate was independent of the tide in the uppermost regimes.

Figure 7 is a plot of flushing rate for the entire SRE, which is a single transport time

scale, versus the river discharge during spring and neap tides. This represented a combined effect of the tide-driven exchanges and gravitational circulation exchanges. The intercept value (F_{int}) provides the tidal exchanges, whereas the amounts in excess of the intercept value (here expressed by G_c) give the gravitational circulation exchanges. The tidal exchanges were dominant during spring tide ($F_{int} > G_c$) and the gravitational circulation exchanges during neap tide ($F_{int} < G_c$). Such combined effect ($F_{int} < G_c$) was noted by Officer and Kester (1991) for the entire Narragansett Bay, which depicts only the general exchange characteristics without differentiating spatial variations.

To more clearly understand the spatial variations in the tide-driven exchanges and gravitational circulation exchanges along the SRE during spring and neap tides, the flushing rate for each estuarine segment was plotted against the river discharge (Fig. 8). The plots of the flushing rate (F) against the river discharge (R) represent the combined effects of tidal exchanges and gravitational circulation exchanges on segments 1 to 5 during spring and neap tides. The tidal and gravitational circulation components were comparable in these segments. Only the gravitational circulation exchanges were dominant in segment 6, which is governed by the river flow, during spring and neap tides.

Tide-driven exchanges became dominant over gravitational circulation exchanges near the mouth (SEG1 and SEG2) during spring tide, caused by the larger tidal amplitude of the spring cycle (Fig. 9a). McCarthy (1993) and Savenije (2005) reported that the gravitational circulation is weak near the mouth of exponentially varying estuary, and tide-induced exchange is dominant. On the basis of the stratification parameter, well-mixed conditions were also found near the mouth of the SRE during spring tide (Shaha and Cho, 2009), where the large tidal amplitude enhanced the turbulent mixing. Moreover, the tidal dominancy appeared in the observations of the variations in the diurnal salinity taken at CTD station 7 with low ($28\,m^3\,s^{-1}$) and high ($128\,m^3\,s^{-1}$) river discharges during spring tide, as shown in Fig. 2. In both river discharge cases, the same salinity of 27 psu appeared at CTD station 7 during high tide (Fig. 2a and b). This indicates that the tide was dominant in pushing the salinity of 27 psu from Gwangyang

Bay to the observation point, where the freshwater input was negligible.

In contrast, the gravitational circulation exchanges dominated in the central and inner regimes (SEG3, SEG4 and SEG5) during spring tide (Fig. 9a), where the SRE was partially stratified on the basis of the stratification parameter (Shaha and Cho, 2009) and also as a function of potential energy anomaly. As the M_2 tidal amplitude decreased by 12% within the estuary relative to the mouth (Table 1), the consequent reduction in the vertical mixing enhanced gravitational circulation. Due to the decrease in the tidal amplitude, the gravitational circulation has intensified in the Ariake Bay (Yanagi and Abe, 2005).

The weaker turbulence during neap tide accelerated the gravitational circulation exchanges in all segments of the SRE (Fig. 9b). As a consequence, strong stratification occurred during neap tide in all seasons (Figs. 3c–d and 4e–h). This indicates that the gravitational circulation exchanges were strongly linked to both the stratification and the tide (neap). Strong stratified conditions were also found during neap tide along the SRE as a function of the stratification parameter (Shaha and Cho, 2009) and the potential energy anomaly in the water column. Pulsing of stratification and gravitational circulation is easily understood in terms of the significant reduction in vertical mixing during neap tide due to the weakened effect of the bottom friction (Monismith et al., 1996).

The estuarine parameter $\boldsymbol{\nu}$ (Hansen-Rattray parameter), as determined from Eq. (5), supports that this calculation was reasonable. On the basis of the estuarine parameter $\boldsymbol{\nu}$ (Table 2), the tidal exchanges dominated near the mouth, whereas the gravitational circulation exchanges dominated at the upstream end (SEG6). Figure 10 shows a plot of the estuarine parameter against the river discharge. The SRE was dominated by tidal exchanges at low river flows ($<20\,m^3\,s^{-1}$). For average to high river flows, the contributions of tidal and gravitational circulation exchanges were of comparable magnitude.

5 Discussion

5.1 Exchange processes based on potential energy anomaly

The horizontal density gradient has important implications in generating tidally varying stratification and gravitational circulation (Savenije, 2005). Strong stratification events are periods of intense gravitational circulation (Monismith, 1996) which are linked through straining of the salinity field. Tidal straining is the result of velocity shear acting on a horizontal density gradient creating oscillations in the stratification of the water column (Murphy et al., 2009). To determine the influence of tidal straining on water column stratification, which is strongly linked with gravitational circulation, the potential energy anomaly ϕ of the water column for each CTD cast was calculated. Following the approaches of Simpson et al. (1990) and de Boer et al. (2008), the potential energy anomaly is the amount of work necessary to completely mix the water column ($\mathrm{J\,m^{-3}}$) which can be calculated from

$$\phi = \frac{1}{H}\int_{-H}^{0} gz(\overline{\rho}-\rho)dz \tag{6}$$

with the depth average density

$$\overline{\rho} = \frac{1}{H}\int_{-H}^{0} \rho dz \tag{7}$$

where ρ is the vertical density profile over the water column of depth H, z is the vertical co-ordinate and g is the gravitational acceleration ($9.8\,\mathrm{ms^{-2}}$). For a given density profile, ϕ ($\mathrm{J\,m^{-3}}$) represents the amount of work required to completely mix the water column.

Variations in the tidal exchanges and gravitational circulation exchanges naturally arise through neap-spring variations in the presence of the potential energy anomaly

along the SRE. Figure 11 depicts the spatial variation in the potential energy anomaly ϕ during spring and neap tides along the SRE. Each contour of the spring and neap tides was the average for 12 samples obtained from August 2004 to April 2007. The strength of tide-driven mixing and stratification varied significantly between the spring and neap tides, up to approximately 20 km landward, as a function of ϕ.

The amount of ϕ was less than 10 J m^{-3} during spring tide near the mouth (landward 7 km) of the SRE due to tidally driven turbulent mixing (Fig. 11). Burchard and Hofmeister (2008) have examined the dynamics of the potential energy anomaly at a location, where the water column is fully destabilized during flood, with a range of ϕ between 0 and 9 J m^{-3}. Therefore, it can be assumed that tide-driven exchanges may have dominant, when ϕ is <10 J m^{-3}. In addition, the tidal exchange zone extends roughly a tidal excursion from the mouth (Signell and Butman, 1992). The median tidal excursion observed in the SRE was 6.8 km (Shaha and Cho, 2009), that indicating the tidal exchange zone. Signell and Butman (1992) also found rapid exchange in the tidal mixing zone. As per the stratification parameter, well-mixed conditions were found near the mouth (landward about 7 km) of the SRE during spring tide (Shaha and Cho, 2009), that also indicating the tidal exchange zone. Thus the tidal dominant exchange zone, as determined from the flushing rate near the mouth (SEG1 and SEG2) during spring tide, is consistent well with the function of ϕ, stratification parameter and tidal excursion.

In contrast, the amount of ϕ increased to 10~24 J m^{-3} during spring tide landward of 7 km from the mouth (Fig. 11), where gravitational circulation exchanges dominated over tidal exchanges (Fig. 9a). The water column contained more ϕ in the central and inner regimes of the SRE relative to the mouth due to the reduction in mixing as the M_2 tidal amplitude decreased by 12% within the estuary (Table 1). As a consequence, gravitational circulation exchanges dominated over tide-driven exchanges in the central and inner regimes of the SRE.

Increased values of ϕ in the water column (27< ϕ <67 J m^{-3}) represents stronger stratification during neap tide than during spring tide. The weaker turbulence during a

neap tide could lead to the reduction in mixing and the consequent increase of ϕ in the water column enhanced gravitational circulation in all segments (Fig. 9b). The dynamics of the potential energy anomaly has examined by Burchard and Hofmeister (2008) on a strongly stratified water column, where gravitational circulation exchange exists over the whole tidal period, with a range of ϕ between 45 and 60 J m^{-3}. The link between stratification and gravitational circulation develops during neap tide due to the significant reduction in vertical mixing, which is the result of the weakened bottom friction (Nunes Vaz et al. 1989; Monismith et al., 1996).

There was no substantial amount of ϕ required to completely mix the water column landward of 20 km from the mouth of the SRE (SEG6), where only the gravitational circulation exchange was dominant during spring and neap tides (Fig. 9a and b). This also indicates that the tidal effects decreased at landward of 20 km from the mouth and the combined effects between tidal exchanges and gravitational circulation exchanges start from this location. Thus, the tidal exchange and gravitational circulation exchange, calculated using the flushing rate, showed well consistency with the function of potential energy anomaly.

5.2 Effects of exchange processes on spatial heterogeneity of Chlorophyll a

A single transport time scale, the flushing rate for the entire SRE, could not provide information about the connections between the transport and spatial heterogeneity of non-conservative quantities such as chlorophyll a. Conversely, the calculation of the flushing rate for multiple segments of the SRE provided strong clues about the importance of transport processes in shaping the spatial patterns of chlorophyll a. Park et al., (2005) conducted a study on spatiotemporal fluctuations in the abundance of the demersal copepod, *Pseudodiaptomus* sp., in the SRE during spring tide. They used six fixed sampling stations, with a distance of approximately 4 km, from the head to the estuary mouth. Each station of their study was incorporated to each estuarine segment in this study.

The chlorophyll a concentrations measured during their research period are shown

in Table 3. The concentrations were lowest at SEG6 which was only governed by the gravitational circulation exchange. As gravitational circulation exchange may increase in strength with increasing river flow, advective transport of estuarine resident populations will increase (Monismith et al., 2002). Owing to this advective loss, the chlorophyll a concentration was lowest in SEG6. However, the chlorophyll a concentration was highest in SEG5 due to advection by the river flow from SEG6. This region is the landward limit of haline stratification as a function of ϕ where there is no net landward and seaward movement of water. As a result, *Pseudodiaptomus* sp. maintained their positions in SEG5.

Conversely, lower concentration of chlorophyll a was also found at CTD station 3, located near the mouth of the SRE. Strong tide-driven exchange was found in SEG1 during spring tide (Fig. 9a), which caused advection of planktonic organisms from the mouth of the SRE to Gwangyang Bay. As a result, the concentration was lower near the mouth. Hydrodynamic conditions, such as tide-driven exchanges and gravitational circulation exchanges, are entirely different during spring and neap tides in the SRE. Therefore, a study on the abundance of the demersal compepod *Pseudodiaptomus* sp. should conduct during neap tide, as the SRE is strongly stratified during neap tide that inhibits vertical migration of planktonic organisms.

6 Conclusions

The flushing rate for the entire SRE showed the general exchange characteristics without identifying spatial variations. To investigate spatial and spring-neap variations of gravitational circulation and tide-driven exchanges the flushing rate was calculated for multiple segments of the SRE. The tides caused rapid exchange in the vicinity of the mouth during spring tide compared to neap tide. The stratification and water column stability was found to vary in different sections of the SRE as a function of potential energy anomaly which modulated gravitational circulation and tide-driven exchanges. The significant reduction in vertical mixing during neap tide made a strong coupling be-

tween stratification and gravitational circulation. The tidal exchanges dominated near the mouth during spring tide due to the larger tidal amplitude where gravitational circulation was weaker. Gravitational circulation induced in the central and inner regime during spring tide due to the reduction in tidal amplitude that caused partially stratified conditions. Gravitational circulation only dominated at the upstream end governed by the river flow during both spring and neap tides. These results furnished strong clues about the spatially varying abundance of planktonic organisms in the SRE. Results suggested the use of spatially varying flushing rate to estimate tide-driven and gravitational circulation exchanges, and also to understand the distributions of living biomass and suspended particles in an estuary.

Acknowledgements. This research was supported by the NAP program of the Korea Ocean Research Development Institute. The authors would like to acknowledge the members of the Earth Environment Prediction Laboratory for their enthusiastic supports during the data collection.

References

Bae, D. H., Jung, I. W., and Chang, H.: Long-term trend of precipitation and runoff in Korean river basins, Hydrol. Process., 22, 2644–2656, 2008.

Bell, C., Vassie, J. M., and Woodworth, P. L.: POL/PSMSL Tidal Analysis Software Kit 2000 (Task-2000), Permanent Service for Mean Sea Level, CCMS Proudman Oceanographic Laboratory, Bidston Observatory, Birkenhead, UK, 20 pp., 1999.

Burchard, H. and Hofmeister, R.: A dynamic equation for the potential energy anomaly for analysing mixing and stratification in estuaries and coastal seas, Estuar. Coast. Shelf S., 77, 679–687, 2008.

de Boer, G. J., Pietrzak, J. D., and Winterwerp, J. C.: Using the potential energy anomaly equation to investigate tidal straining and advection of stratification in a region of freshwater influence, Ocean Model., 22, 1–11, 2008.

deCastro, M., Gomez-Gesteira, M., Prego, R., and Alvarez, I.: Ria-ocean exchange driven by tides in the Ria of Ferrol (NW Spain), Estuar. Coast. Shelf S., 61, 15–24, 2004.

Dyer, K. R.: Estuaries, A Physical Introduction, John Wiley, London, UK, 2nd edn., 195 pp., 1997.
Geyer, W. R.: The importance of suppression of turbulence by stratification on the estuarine turbidity maximum, Estuaries, 16, 113–125, 1993.
Hansen, D. V. and Rattray, R.: Gravitational circulation in straits and estuaries, J. Mar. Res., 23, 104–122, 1965.
Hansen, D. V. and Rattray, R.: New dimensions in estuary classification, Limnol. Oceanogr., 11, 319–326, 1966.
Hough, A. R. and Naylor, E.: Field studies on retention of the planktonic copepod Eurytemora affinis in a mixed estuary, Mar. Ecol. Prog. Ser., 76, 115–122, 1991.
Jassby, A. D., Kimmerer, W. J., Monismith, S. G., Armor, C., Cloern, J. E., Powell, T. M., Schubel, J. R., and Vendlinski, T. J.: Isohaline position as a habitat indicator for estuarine populations, Ecol. Appl., 5, 272–289, 1995.
Jay, D. A. and Smith, J. D.: Circulation, density structure and neap-spring transitions in the Columbia River Estuary, Prog. Oceanogr., 25, 81–112, 1990.
Ji, Z. G.: Hydrodynamics and Water Quality: Modeling Rivers, Lakes and Estuaries, John Wiley, New Jersey, USA, 1st edn., 676 pp., 2008.
Kimmerer, W. J., Burau, J. R., and Bennett, W. A.: Persistance of tidally-oriented vertical migration by zooplankton in a temperate estuary, Estuaries, 25, 359–371, 2002.
Kimmerer, W. J., Burau, J. R., and Bennett, W. A.: Tidallyoriented vertical migration and position maintenance of zooplankton in a temperate estuary, Limnol. Oceanogr., 43, 1697–1709, 1998.
Monismith, S. G., Burau, S. R., and Stacey, M.: Stratification dynamics and gravitational circulation in northern San Francisco Bay, edited by: In J. T. Hollibaugh, San Francisco Bay: The Ecosystem, American Association for the Advancement of Science, San Francisco, California, 123–153, 1996.
Monismith, S. G., Kimmerer, W., Stacey, M. T., and Burau, J. R.: Structure and Flow-Induced Variability of the Subtidal Salinity Field in Northern San Francisco Bay, J. Phys. Ocean , 32, 3003–3019, 2002.
Monsen, N. E, Cloern, J. E., Lucas, L. V., and Monismith, S. G.: A comment on the use of flushing time, residence time, and age as transport time scales, Limnol. Oceanogr., 47, 1545–1553, 2002.
Morgan, C. A., Cordell, J. R., and Simenstad, C. A.: Sink or swim? Copepod population

maintenance in the Columbia River estuarine turbidity-maxima region, Mar. Biol., 129, 309–317, 1997.
Murphy, P., Waterhouse, A., Hesser, T., Penko, A., and Valle-Levinson, A.: Subtidal flow and its variability at the entrance to a subtropical lagoon, Cont. Shelf Res., 29, 2318–2332, 2009.
Nunes Vaz, R. A., Lennon, G. W., and de Silva Samarasinghe, J. R.: The negative role of turbulence in estuarine mass transport, Estuar. Coast. Shelf S., 28, 361–377, 1989.
Officer, C. B. and Kester, D. R.: On estimating the non-advective tidal exchanges and advective gravitational circulation exchanges in an estuary, Estuar. Coast. Shelf S., 32, 99–103, 1991.
Park, E. O., Suh, H. L., and Soh, H. Y.: Seasonal variation of the abundance of the demersal copepod *Pseudodiaptomus* sp. (Calanoida, Pseudodiaptomidae) in the Seomjin River Estuary, South Korea, Korean J. Environ. Biol., 23, 367–373, 2005.
Pilson, M. E. Q.: On the residence time of water in Narragansett bay, Estuaries, 8, 2–14, 1985.
Press, W. H., Flannery, B. P., Teukolsky, S. A., and Vetterling, W. T.: Numerical Recipes in C, Cambridge University Press, Cambridge, UK, 1st edn., 768 pp., 1988.
Ribeiro, C. H. A., Waniek, J. J., and Sharples, J.: Observations of the spring-neap modulation of the gravitational circulation in a partially mixed estuary, Ocean Dyn., 54, 299–306, 2004.
Savenije, H. H. G.: Salinity and Tides in Alluvial Estuaries, 1st edn., Elsevier, Amsterdam, The Netherlands, 197 pp., 2005.
Shaha, D. C. and Cho, Y.-K.: Comparison of empirical models with intensively observed data for prediction of salt intrusion in the Sumjin River estuary, Korea, Hydrol. Earth Syst. Sci., 13, 923–933, 2009, http://www.hydrol-earth-syst-sci.net/13/923/2009/.
Sheldon, J. E. and Alber, M.: A comparison of residence time calculations using simple compartment models of the Altamaha River Estuary, Georgia, Estuaries, 25, 1304–1317, 2002.
Sheldon, J. E. and Alber, M.: The calculation of estuarine turnover times using freshwater fraction and tidal prism models: a critical evaluation, Estuar. Coast., 29, 133–146, 2006.
Signell, R. P. and Butman, B.: Modeling tidal exchange and dispersion in Boston Harbor, J. Geophys. Res., 97, 15591–15606, 1992.
Simpson, J. H., Brown, J., Matthews, J., and Allen, G.: Tidal straining, density currents and stirring control of estuarine circulation, Estuaries, 13, 125–132, 1990.
Uncles, R. J. and Stephens, J. A.: Salt intrusion in the Tweed Estuary, Estuar. Coast. Shelf S., 43, 271–293, 1996.
Uncles, R. J., Elliott, R. C. A., and Weston, S. A.: Observed fluxes of water, salt and suspended

sediment in a partially mixed estuary, Estuar. Coast. Shelf S., 20, 147–167, 1985.
West, J. R. and Broyd, T. W.: Dispersion coefficients in estuaries, P. I. Civil Eng., 71, 721–737, 1981.
Williams, B. L.: Flushing time calculations for the Upper Waitemata Harbour, New Zealand, New Zeal. J. Mar. Fresh., 20, 455–465, 1986.
Yanagi, T. and Abe, R.: Increase in water exchange ratio due to a decrease in tidal amplitude in Ariake Bay, Japan, Cont. Shelf Res., 25, 2174–2181, 2005.

Table 1. Observed tidal amplitudes for M_2, S_2, K_1 and O_1 at the Gwangyang and Hadong tidal stations.

Tidal station	Amplitude (cm)			
	M_2	S_2	K_1	O_1
Gwangyang (GT2)	109.3	46.7	18.7	14.3
Hadong (HT)	96.6	42.8	17.9	11.9

HESSD
7, 1621–1654, 2010

Table 2. Estuarine parameter (ν) during spring and neap tide for various segments.

Station	Estuarine Parameter (ν)	
	Spring	Neap
SEG1	0.99	0.93
SEG2	0.89	0.74
SEG3	0.80	0.78
SEG4	0.72	0.50
SEG5	0.48	0.47
SEG6	0.14	0.04

HESSD
7, 1621–1654, 2010

Table 3. Chlorophyll a concentration in the Sumjin River Estuary (Park et al., 2005).

Station	Chlorophyll a concentration ($\mu g\,L^{-1}$)
CTD23 (SEG6)	2.5~18.2
CTD20 (SEG5)	3.7~108.9
CTD15 (SEG4)	3.0~44.4
CTD11 (SEG3)	3.8~45.2
CTD8 (SEG2)	2.5~48.5
CTD3 (SEG1)	2.8~23.7

HESSD
7, 1621–1654, 2010

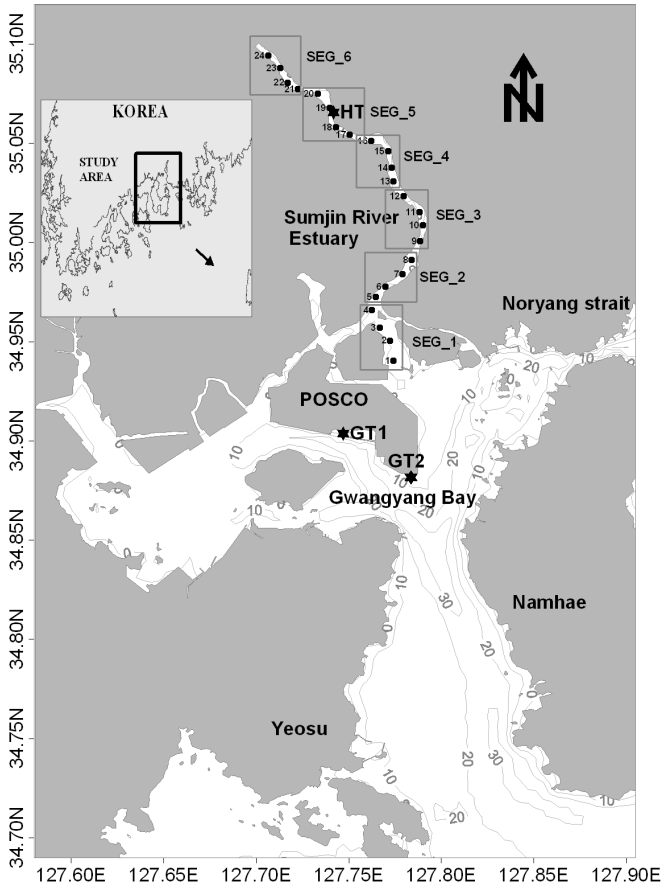

Fig. 1. Map of the study area. The solid circles indicate the CTD stations. The star mark denotes the locations of the Gwangyang (GT1 and GT2) and Hadong (HT) tidal stations.

HESSD
7, 1621–1654, 2010

Flushing rate for gravitational circulation and tidal exchanges

D. C. Shaha et al.

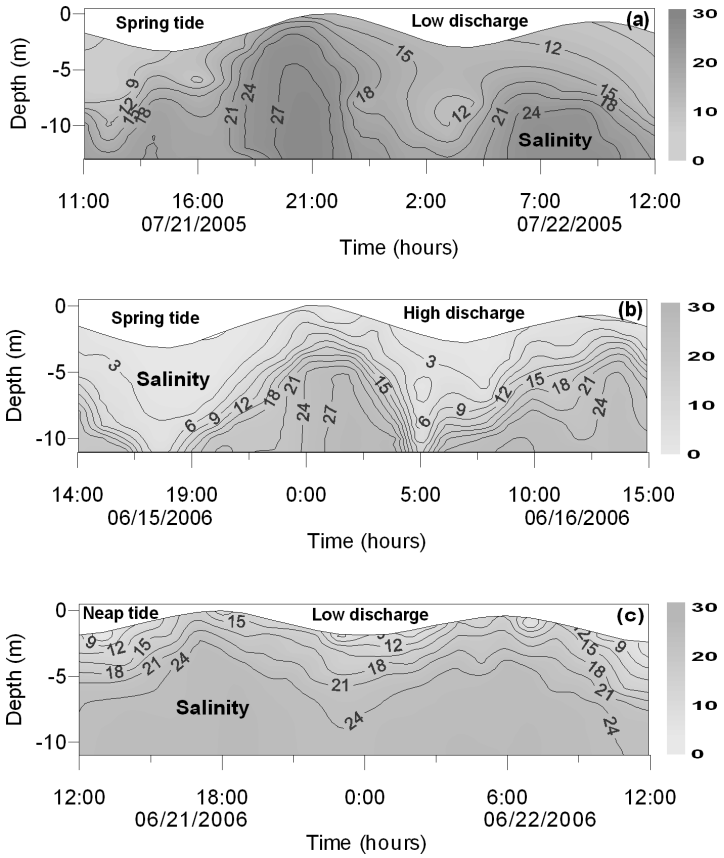

Fig. 2. Time-depth distributions of the salinity profile during spring tide, with low river discharge ($28\,m^3\,s^{-1}$) for 21–22 July 2005 **(a)**, during spring tide, with high river discharge ($120\,m^3\,s^{-1}$) for 15–16 June 2006 **(b)**, and during neap tide, with low river discharge ($18\,m^3\,s^{-1}$) for 21–22 June 2006 **(c)** over a tidal cycle at station 7.

HESSD
7, 1621–1654, 2010

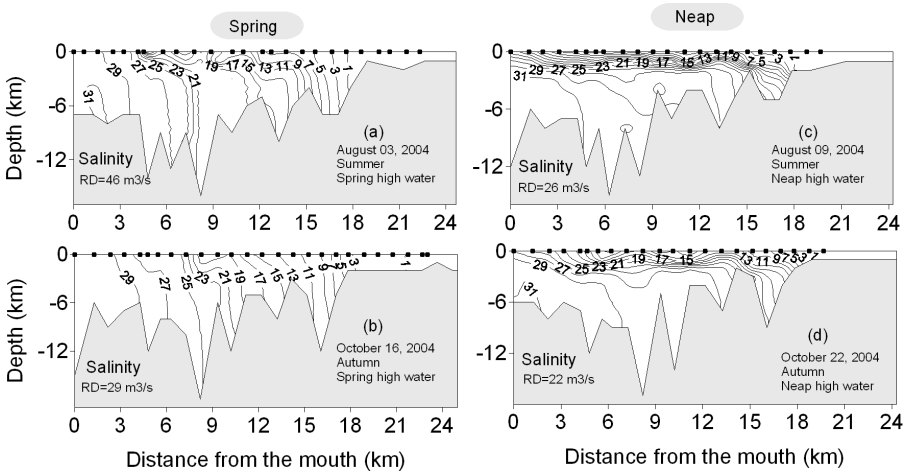

Fig. 3. Salinity distributions for all longitudinal depth surveys of the Sumjin River Estuary at high water during spring **(a, b)** and neap **(c, d)** tides during summer and autumn of 2004. The black solid circles indicate the CTD stations.

HESSD
7, 1621–1654, 2010

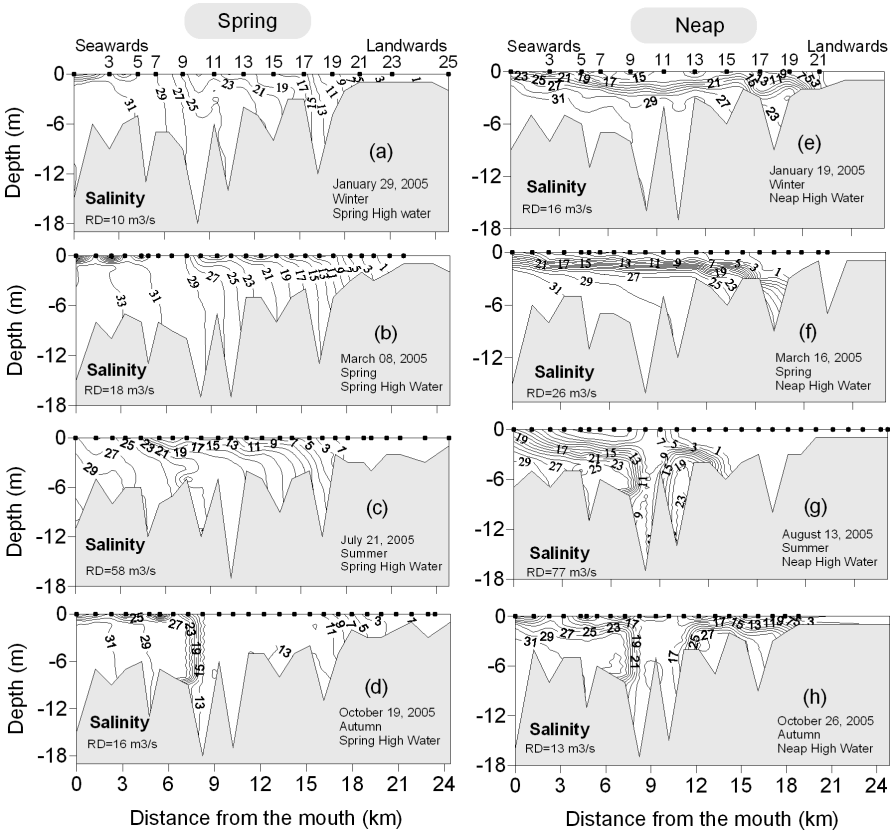

Fig. 4. Salinity distributions for all longitudinal depth surveys of the Sumjin River Estuary at high water during spring **(a, b, c, d)** and neap **(e, f, g, h)** tides in each season of 2005. The black solid circles indicate the CTD stations.

HESSD
7, 1621–1654, 2010

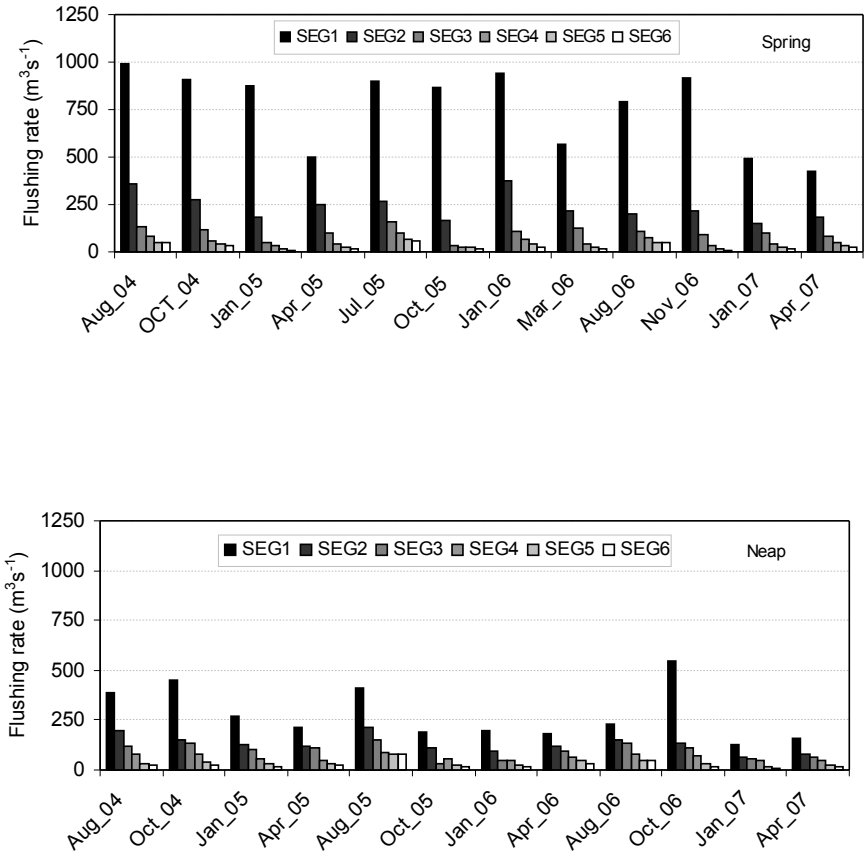

Fig. 5. Temporal variation of the flushing rate ($m^3 s^{-1}$) among six segments during spring and neap tides.

HESSD
7, 1621–1654, 2010

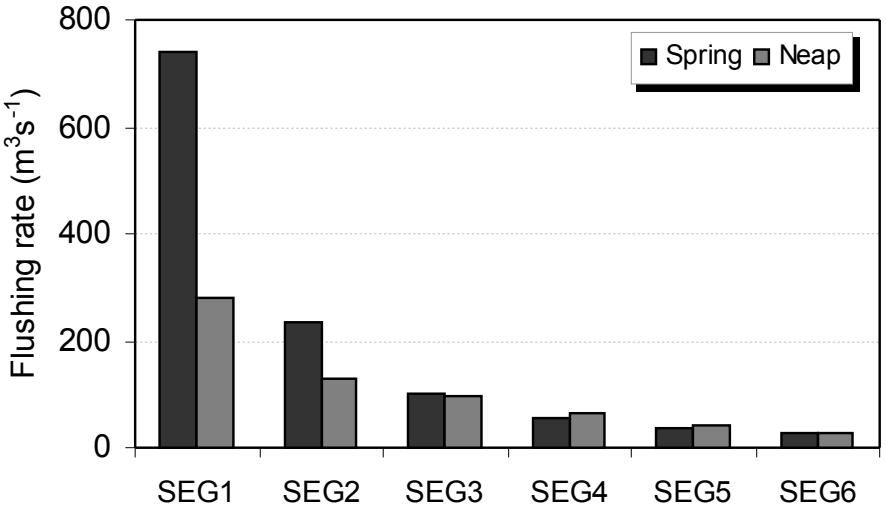

Fig. 6. Spatial variation of the mean flushing rate ($m^3\ s^{-1}$) during spring and neap tides.

HESSD
7, 1621–1654, 2010

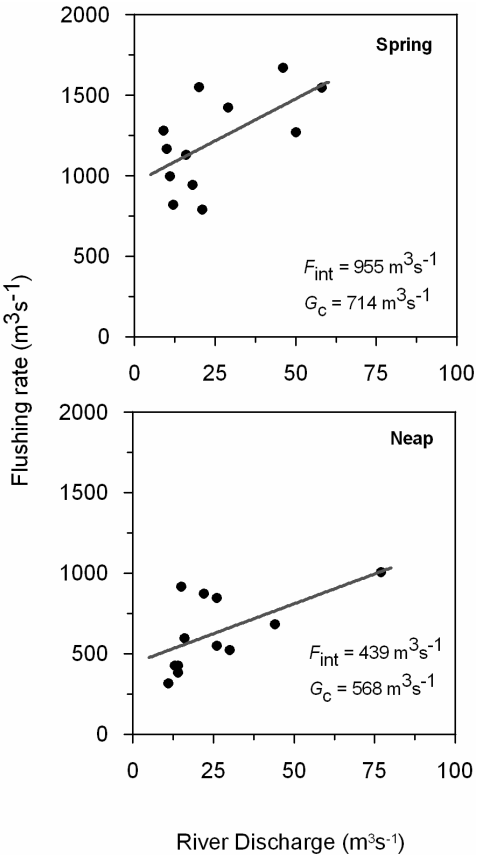

Fig. 7. Plot of the flushing rate (F) calculated for the entire Sumjin River Estuary against the river discharge (R) during spring and neap tides. The intercept value, F_{int}, denotes the tidal exchanges. The amounts in excess of F_{int} indicate the gravitational circulation exchanges (G_c).

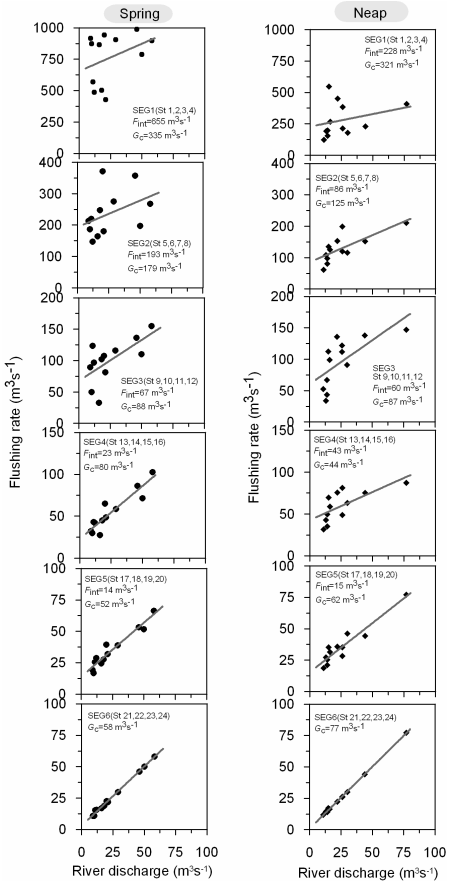

Fig. 8. Plot of the flushing rate (F) against the river discharge (R) for various segments of the Sumjin River Estuary during spring (left panel) and neap (right panel) tides. The intercept value, F_{int}, indicates the tidal exchanges. The amounts in excess of the F_{int} value (here expressed by G_c) indicate gravitational circulation exchanges. Only the gravitational circulation exchanges dominated on segment 6, where the fitting line is linear, with an intercept at zero, where the F value increases with increasing R value.

HESSD
7, 1621–1654, 2010

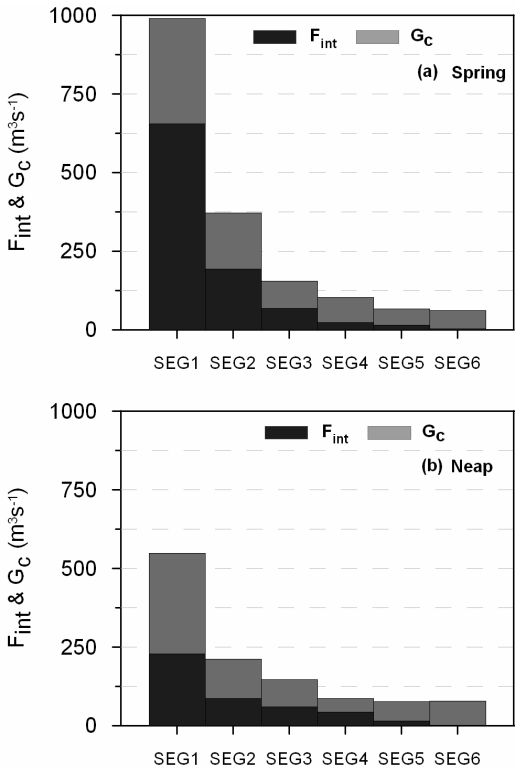

Fig. 9. Combined effects of tidal exchanges (F_{int}) and gravitational circulation exchanges (G_c) in each estuarine segment of the Sumjin River Estuary during spring (upper) and neap (lower) tides. Only the gravitational circulation exchanges dominated in segment 6, which were governed by the river flow during spring and neap tides.

HESSD
7, 1621–1654, 2010

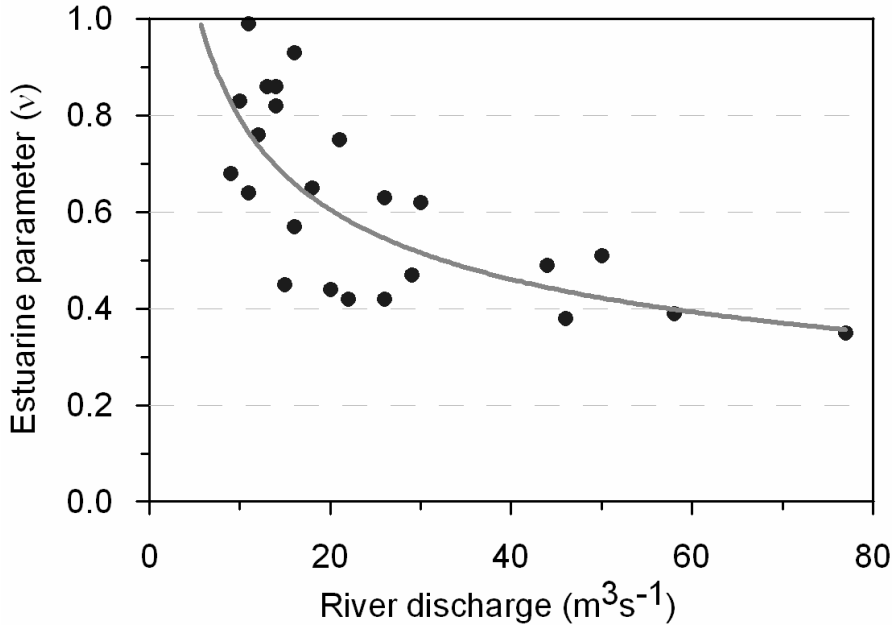

Fig. 10. Plot of the estuarine parameter versus the river discharge for the Sumjin River Estuary.

HESSD
7, 1621–1654, 2010

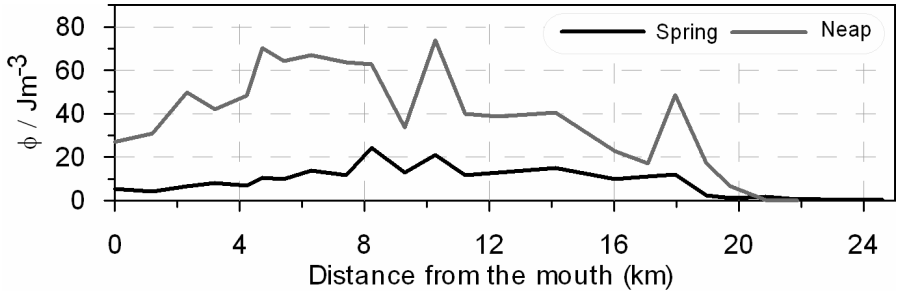

Fig. 11. Spatial variation in the potential energy anomaly during spring and neap tides along the Sumjin River Estuary. Each contour is the average of twelve samples obtained from August 2004 to April 2007.

HESSD

7, 1621–1654, 2010